JOURNAL OF MATERIALS SCIENCE **35** (2000) 3433–3440

Improvements of the microstructure and erosion resistance of boron carbide with additives

P. LARSSON, N. AXÉN, S. HOGMARK
Uppsala University, The Ångström Laboratory, Department of Materials Science, Box 534, S-751 21 Uppsala, Sweden
E-mail: peter.larsson@material.uu.se

A series of test materials were produced from boron carbide (B_4C) powders with additions of either boron in amounts up to 60 wt.%, silicon (4 wt.%) or silicon and silicon carbide (4 wt.% and 30 wt.%, respectively). The powder mixtures were densified by encapsulation hot-isostatic pressing. The test materials where evaluated in dry particle erosion tests with silicon carbide grits. Particular attention was given to the relation between the microstructure and the composition. It was found that boron additions up to 20 wt.%, decreased the average grain size and reduced the porosity of the boron carbide. A material with 60 wt.% boron exhibited very low porosity and supreme resistance to particle erosion. The erosion resistance was also significantly improved by additions of silicon and silicon carbide. The favorable effects of boron, silicon and silicon carbide are discussed in terms of their influence on microstructural parameters, such as grain size, porosity, grain boundaries and reduction of free carbon.

1. Introduction

As an engineering material, boron carbide (often B_4C) offers excellent properties such as low density, high melting point, high elastic modulus and extreme hardness. Due to its high hardness, boron carbide is highly resistant to erosion and abrasion [1]. Boron carbide is at present employed as a lightweight armor material, high-temperature thermoelectric conversion [2] and in erosive wear applications such as nozzles. However, its usability is limited mainly by its propensity to spalling and poor oxidation resistance.

The common elastic-plastic fracture models [3, 4] of particle erosion, postulate that the wear of brittle materials can be estimated by comparing the erosive particle to a sharp and hard indenter which forces the softer surface to deform with a negligible deformation of the indenter. The equations are based on the approach that the fracture toughness can be used as a measure of the material's resistance to radial cracking, and that the size of the lateral cracks scales with the lengths of the radial cracks. Thus, as the eroded material increases in toughness, the models predict the erosive wear by brittle fracture to decrease.

To assess the different removal mechanisms that may act during particle erosion, it is important to have an understanding of the interaction between the erosive particle and the surface. It is not obvious that the elastic-plastic fracture models are valid when the erosive particles are softer or similar in hardness to the eroded material. The removal mechanisms of ceramics under such conditions may be completely different from those for erosion by harder particles; and it may be suspected that most damage instead would occur at weak spots at the surface, such as partially supported material at edges, grain boundaries and pores. The wear resistance would then rather be attributed to microstructural aspects of the eroded surface, rather than to fracture toughness or hardness of the bulk.

Boron carbide exists in a wide range of compositions between B_4C to $B_{10.5}C$ [5] in the B-C system. The crystallographic structure of boron carbide is rombohedral with 8 boron icosahedra in each corner [6]; the composition of such a unit cell can be written B_6-C-C-C-B_6 or $B_{12}C_3$. Within the row of interstitial atoms an exchange of boron and carbon atoms can take place with the optimally stable composition being B_6-C-B-C-B_6 or $B_{13}C_2$ [7]. It has also been found that there exists a row of boron carbides with somewhat altered formulae, all however with the overall stoichiometry $B_{12}C$ [8].

Densification of pure boron carbide is rather difficult. Previous work has shown that boron carbide undergo considerable microstructural coarsening with little densification during sintering [9, 10–12]. The surface-to-surface mass transport is responsible for the coarsening, which is a natural consequence of mass-transport in the absence of densification. Fine grained compounds of up to 95% theoretical density have been obtained by pressureless sintering from fine powders and by additions of free carbon, which facilitates the sintering [10]. The additive strategy results in sintered materials with residual graphite, which in combination with porosity reduces the strength in comparison to boron carbide produced by hot pressing and hot isostatic pressing. The disadvantage with hot pressing (conducted at about 2200 °C) is the extensive carbon diffusion, which may take place

from the mould towards the sample during sintering. This can be avoided by using an encapsulation technique in combination with hot isostatic pressing, which also allows the sintering to be conducted at lower temperatures of about 1700 °C, at which extensive grain growth is reduced [13]. However, one source of graphite will remain, as all commercial technical boron carbide powders contain some degree of free carbon. The effect of small quantities of graphite within the microstructure of boron carbide to residual porosity and strength is uncertain.

The present study attempts to eliminate the free carbon contained in commercial technical boron carbide powders by additions of boron, silicon and silicon carbide. In addition, the influence of additives on material properties and the erosive wear resistance is investigated.

2. Experimental

2.1. Materials manufacturing

The boron carbide specimens were produced with a commercially available powder of the HP grade from H.C. Starck. The chemical composition of the supplied powder was 75.8 wt.% B, 21.8 wt.% C, 1.0 wt.% O and a total of 1.45 wt.% of other impurities such as Fe, Si and Al. Since the cellular structure cannot contain less than 4 boron atoms per carbon, 3.6 wt.% boron is required to eliminate 1 wt.% carbon. In this way, it is estimated that the powder contains at least 0.7 wt.% free, uncombined carbon. An X-ray diffraction analysis confirmed that the initial powder contained free graphite. The compositions of the powder mixtures were varied by additions of boron, silicon and silicon carbide, as outlined together with their notations in Table I. All the samples, except MBC60B, were shaped and compacted by cold isostatic pressing (CIP) at a pressure of 200 MPa. One major advantage with CIP is that no binder is needed.

To determine the influence of the compaction method a material with 60 wt.% boron (MBC60B) was produced with injection moulding. This powder was prepared by adding 4 wt.% wax as binder. The powder mixture was milled for a few hours in petrolium solution, thereafter dried and further milled in a ball mill for de-agglomeration. De-binding of the moulded body was carried out by evaporation in vacuum at 600°C for 3 h.

All the samples were glas encapsulated and sintered with hot isostatic pressing at 1850 °C for 1 h under a pressure of 160 MPa.

2.2. Microstructural characterisation

X-ray diffraction was conducted with a Siemens diffractometer D500 (Cu K_α radiation $\lambda = 1.5418$ Å) to determine the phase composition of the samples after HIP. Debye-Scherrer technique using least-square calculations calculated the lattice constants. The microstructure characterisation was carried out with SEM microscopy after electrolytic etching in 1% KOH solution, 30 s, 30 V and 1 A/cm^2. A systematic manual point counting procedure for statistically estimating the volume fraction of an identifiable constituent from sections through the microstructure was used to measure the porosity, as described in [14]. The grain size was estimated by a lineal intercept method on SEM micrographs of polished and etched sections at appropriate magnification, a procedure outlined in [15].

2.3. Particle erosion

Erosion tests were conducted in a centrifugal accelerator test rig [16]. The experiments were undertaken with 200 μm silicon carbide grits, an erodent impact velocity of 93 m/s and an impingement angle of 90°. Vickers indentations measured the hardness of the erosive silicon carbide grits to about 2500 kg/mm^2. The wear rate (removed material per dose of erodent) was determined by measuring the mass loss to an accuracy of ± 0.0001 g after successive erosion runs. Before weighing the specimens were cleaned ultrasonically in de-ionised water and dried. Single particle impacts were produced with 600 μm mesh silicon carbide particles. For comparative reasons a commercial hot pressed SiC material was included in the erosion test. The SiC material exhibited a Vickers hardness of 2800 kg/mm^2, a fracture toughness of 5.4 MPam$^{1/2}$, porosity of about 5 vol.% and with purity higher than 99 wt.% of β-SiC.

2.4. Hardness and fracture toughness

Vickers microhardness indentations were made on polished sample surfaces, using a load of 500 g. At this load, all samples exhibited radial cracking. Indentation parameters were set 15 s loading time, and the peak

TABLE I The chemical composition and material properties of the boron carbide specimens

Specimen	Chemical Composition	Grain Size (μm)	Hardness (HV)	Fracture Toughness (MPa m$^{1/2}$)	Porosity (vol.%)
BC	B4C	4.3	3630	4.36	3.0
BC2B	98 wt.% B4C + 2 wt.% B	3.8	3580	4.35	1.1
BC10B	98 wt.% B4C + 10 wt.% B	3.6	3630	4.28	1.0
BC20B	80% B4C + 20% B	2.8	3540	4.15	0.9
BC60B	40 wt.% B4C + 60 wt.% B	80 vol.% 3.0 + 20 vol.% 18.4	3590	4.37	0.1
MBC60B	40 wt.% B4C + 60 wt.% B (mould injected)	80 vol.% 3.3 + 20 vol.% 7.9	3580	4.15	0.1
BCSi	96 wt.% B4C + 4 wt.% Si	B4C 6.0 + SiC 2.2	3570	4.27	0.1
BCSiSiC	66 wt.% B4C + 4 wt.% Si + 30 wt.% SiC	B4C 5.6 + SiC 4.7	3280	4.25	0.1

load held for another 15 s. At least five indentations were made on each material. A formula by Blendell as cited by Ponton and Rawlings [17, 18] was used to calculate the fracture toughness from the length of the radial cracks:

$$K_c = 0.0141\left(\frac{P}{a^{3/2}}\right)\left(\frac{E}{H_V}\right)\log_{10}\left(\frac{8.4a}{c}\right) \qquad (1)$$

where K_c is the fracture toughness, P the indentation load, a the half length of the diagonal of the impression, E Young modulus, H_v the Vickers hardness and c is the radial crack length. The scatter of the hardness tests and the fracture tests were similar for all the materials; and within 5% and 10%, respectively.

3. Results

3.1. Materials

Grain size, hardness, fracture toughness and the residual porosity of the test materials are shown in Table I. Hardness and fracture toughness were not significantly affected by even the higher additions of B or Si. Additions of 30 wt.% SiC reduced the hardness slightly. The average grain size tended to decrease with the boron content up to 20 wt.% B. In the specimens with 60 wt.% boron some grains had grown considerably, and two characteristic ranges of grain sizes were observed. Both the BC60B and the MBC60B specimens showed the same pattern, but the CIP:ed material had a larger average grain size than the one produced with injection moulding.

Effects of boron and silicon additives on the residual porosity are illustrated by the SEM images of polished surfaces in Fig. 1. Pure BC contains a high degree of porosity, and also some larger pores (Fig. 1a). A substantial improvement is seen for the BC2B material, with 2 wt.% boron (Fig. 1b), where no large pores can be distinguished. A similar improvement was exhibited by all boron carbide materials with 10 wt.% and 20 wt.% B. Additions of 60 wt.% boron produced a material with a very low level of porosity (Fig. 1c). Also the additions of Si resulted in comparably low fractions of porosity, less than 0.1 vol.% (Fig. 1d). According to

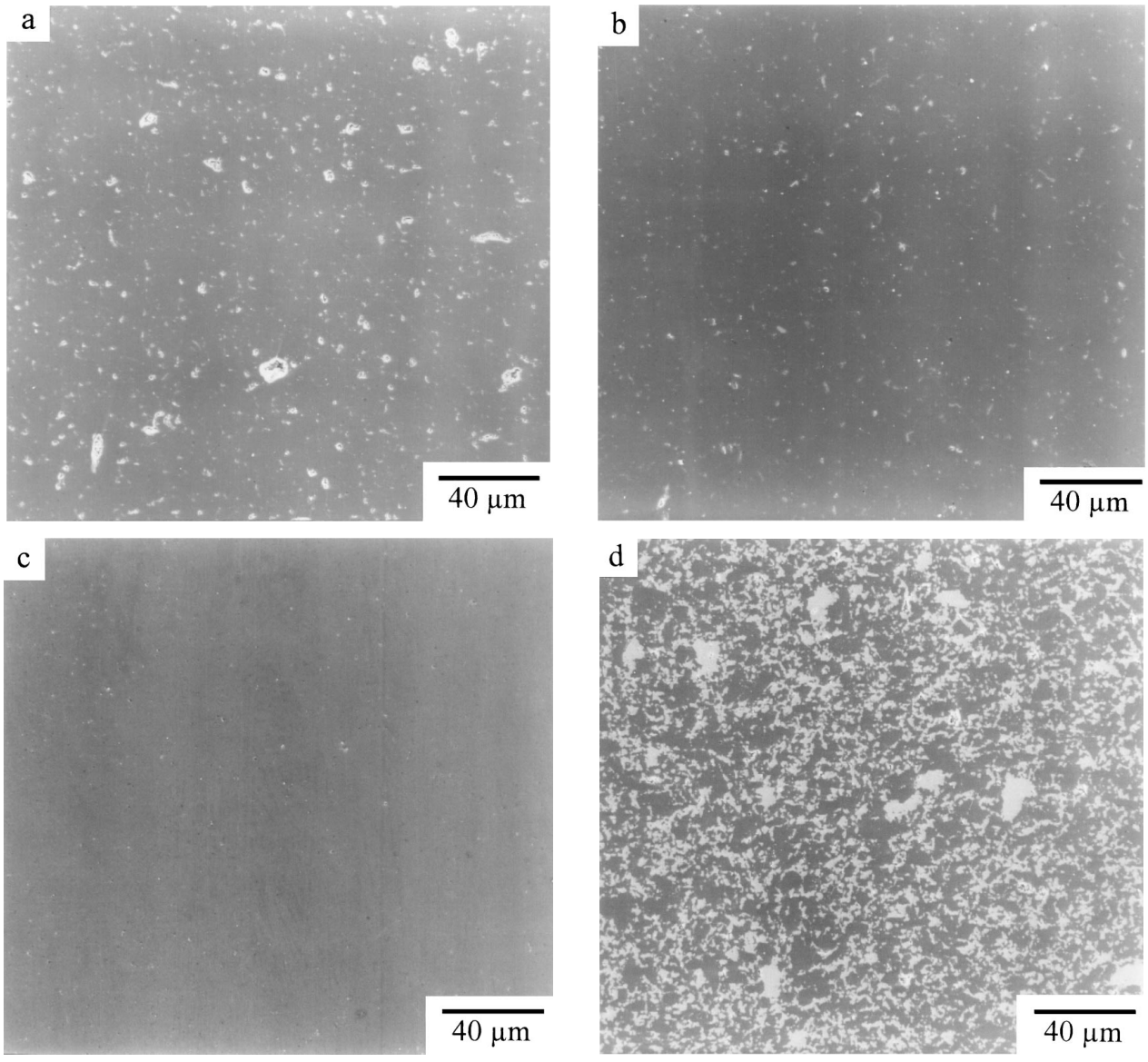

Figure 1 SEM images of polished surfaces on boron carbides with various additions. (a) BC, (b) BC2B, (c) BC60B and (d) BCSiSiC.

TABLE II The composition of the sintered materials according to XRD analysis

Composition \ Specimen	B4C	Graphite	β-SiC
BC	X	X	
BC2B	X	X	
BC10B	X	X	
BC20B	X		
BC60B	X		
MBC60B	X	X	
BCSi	X	X	X
BCSiSiC	X	X	X

TABLE III The hexagonal lattice parameters of the boron carbides with boron additions

Specimen	a_H (nm)	c_H (nm)
BC	0.5611 ± 0.0004	1.211 ± 0.002
BC2B	0.5612 ± 0.0002	1.211 ± 0.003
BC10B	0.5612 ± 0.0004	1.211 ± 0.005
BC20B	0.5612 ± 0.0004	1.211 ± 0.002
BC60B	0.5638 ± 0.0008	1.222 ± 0.002

EDS analysis, the light areas in Fig. 1d are silicon carbide. Similarly, The BCSiSiC specimen with 4 wt.% Si and 30 wt.% SiC also contained low amounts of porosity, but was characterized by larger inclusions of silicon carbide.

Phase compositions of the materials as detected by XRD are given in Table II. Graphite was detected in all of the materials with up to 10 wt.% boron. The etched specimen revealed that the graphite particles were finely dispersed in the microstructure, preferably at the grain boundaries. Surprisingly, despite the high boron content in the mould injected MBC60B specimen, graphite could still be readily detected. In the BCSi specimen a reaction bonded SiC phase had formed. Some free graphite was found also in this sample, but no residual silicon and no compounds of silicon and boron could be detected. Similar observations were made in the BCSiSiC material. Hexagonal lattice parameters of the CIP:ed materials with boron additions were calculated from the XRD analyses, see Table III. These results confirm that the a_H and c_H parameters increase with boron content.

3.2. Particle erosion

Boron additions of up to 20 wt.% caused no clear effect on the erosion rates, see Fig. 2. All of the boron carbide materials displayed much better erosion resistance than that of commercial hot pressed SiC. The introduction of Si and SiC in the microstructure of the BCSi and the BCSiSiC materials reduced the erosion rates to less than half of that of pure boron carbide. However, 60 wt.% boron increased the resistance to erosion most remarkably, with the BC60B specimen being the very best with erosion rates about a tenth of those obtained for the pure boron carbide.

The rough surface morphology given in Fig. 3a is representative for the wear scars on the boron carbides

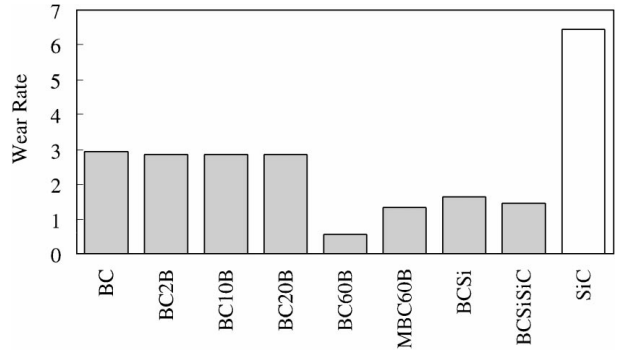

Figure 2 Erosive wear rates obtained at 90° impingement angle, 200 μm silicon grits and 93 m/s impact velocity. The white column illustrates the erosion rate of the reference material.

with up to 20 wt.% boron and seems to be largely the result of intergranular fracture leading to grain pull-out. The eroded surface of BCSiSiC is characterized by irregular crack patterns, presumably formed by small scale fracture, see Fig. 3b. Similar wear scar morphology was produced on the BCSi specimen. In contrary, the wear scar on the BC60B specimen is characterized by a smoother surface with some indications of plastic deformation. Interestingly, there is no evidence of grain pull-out, see Fig. 3c. However, the mould injected MBC60B specimen exhibits a wear scar morphology similar to that of the boron carbides with boron additions up to 20 wt.%, see Fig. 3d.

The single impact damage on the BC10B seen in Fig. 4a is representative of all of the boron carbides with boron addition up to 20 wt.%. It is similar to that damage prescribed by the quasi-static indentation theory, with lateral cracking being the major cause of material loss and with some evidence of radial cracks. In comparison, the lateral fractures for the materials containing Si and SiC are smaller, as exemplified in Fig. 4b. The size of the lateral cracks decreases significantly with the addition of 60 wt.% boron in the BC60B specimen, see Fig. 4c. Investigation of the single impact sites on the mould injected MBC60B specimen (Fig. 4d) revealed that the majority of the lateral fractures were of the same magnitude as the impact sites on the corresponding CIP produced material composition. However, approximately 20% were considerably larger, presumably illustrating a deteriorating effect by graphite inclusions.

4. Discussion

4.1. Material structure

Encapsulation hot isostatic pressing with a fluid as hydrostatic pressure transmitter is the best available pressure-aided densification process [19]. The high pressure provides a high driving force for material transport during sintering which allows the densification to proceed at considerably lower temperatures in comparison to that of traditional sintering. In addition, particularly during the initial stages of the process, the high pressure induces particle rearrangement and high stresses at the particle contact points. Despite the favorable sintering conditions, some fraction of closed

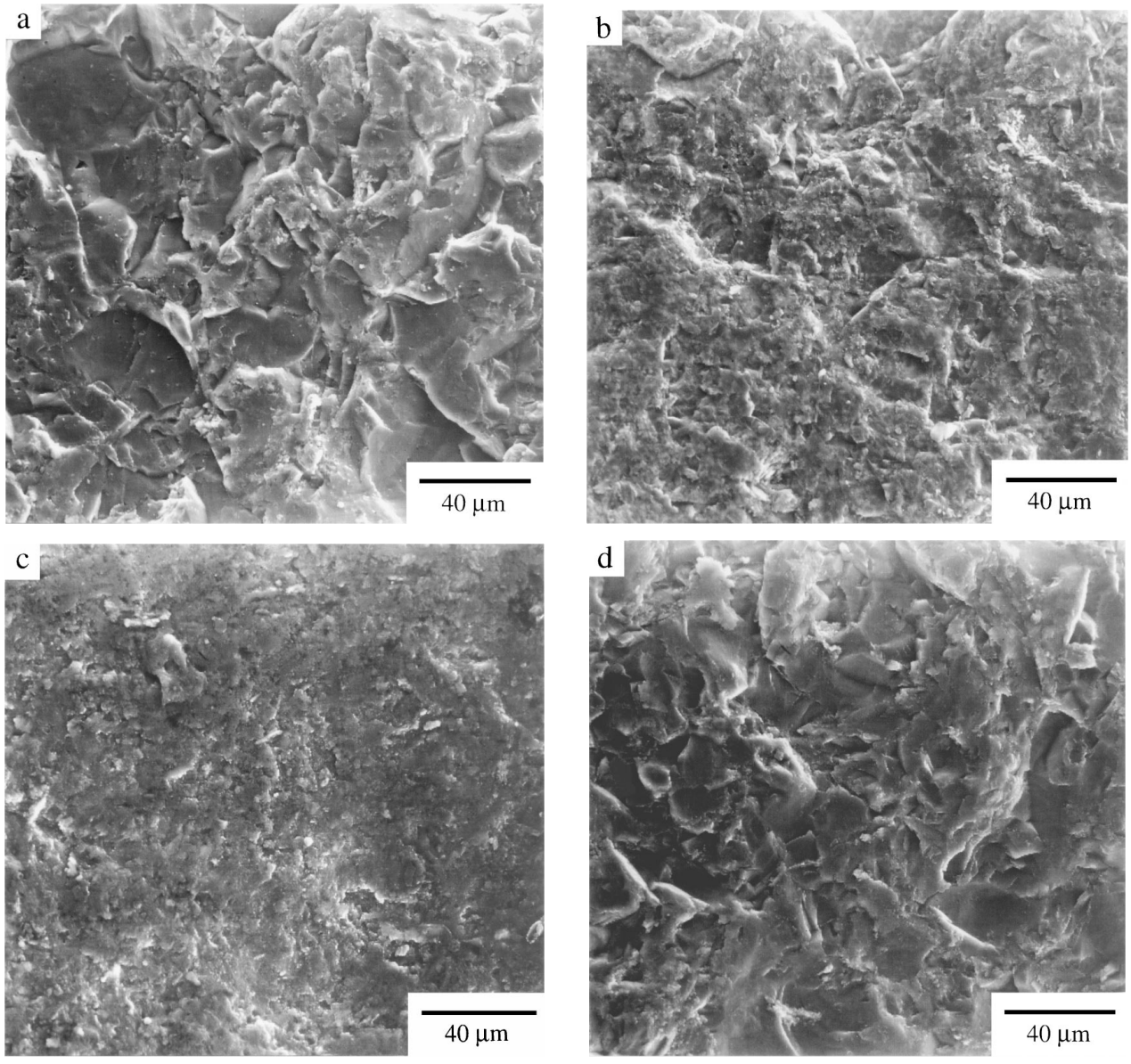

Figure 3 The eroded surfaces of the boron carbide specimens obtained at 90° impingement angle, 200 μm silicon grits and 93 m/s impact velocity: (a) BC, (b) BCSiC, (c) BC60B and (d) MB60B.

porosity still remained in the microstructure of the boron carbide compounds with boron additions up to 20 wt.%. Additives or impurities are generally considered to be advantageous by bringing about a variety of mechanisms to aid the densification process. Although their precise role is not clear it is possible to make certain assumptions.

Presence of free carbon in the powder may have some beneficial effects on the sintering properties of boron carbide. Carbon has been reported to decrease the melting point in the B_4C-C interface to the eutectic point and thereby enhance material transport [20]. Free carbon in the boron carbide powder migrates with the grain boundaries during sintering and is finally agglomerated as graphite at the grain corners. In addition, free graphite dispersions at grain boundaries play an important role in controlling mobility of the grain boundaries [21]. A high driving force is required for the grain boundaries to cross over the graphite particles; the energy is possibly only sufficient in large grains. This is presumably the reason for the smaller grain size distribution in MBC60B containing residual graphite compared to that of the graphite free BC60B specimen.

The amount of closed porosity decreased noticeably in the boron carbide with the addition of only 2 wt.% B compared to the boron carbide without additives. In agreement with other studies [22, 23] this suggests that an effective method to promote sintering in boron carbide is to alter its chemical composition. Boron is an effective sintering aid due to the fact that an exchange of boron and carbon atoms can take place in the row of interstitial atoms in the boron carbide rombohedron. Introduction of boron will cause deviations from the stoichiometry and thereby establish an increased concentration of structural vacancies, through which boron and carbon transitions are possible. This may increase the diffusional mobility of boron and carbon, which results in lattice distortion, in a reduction of the bonding energy and in an activation of the diffusional mechanisms of mass-transport. Since volume diffusion is the most important sintering process for pore shrinkage, the

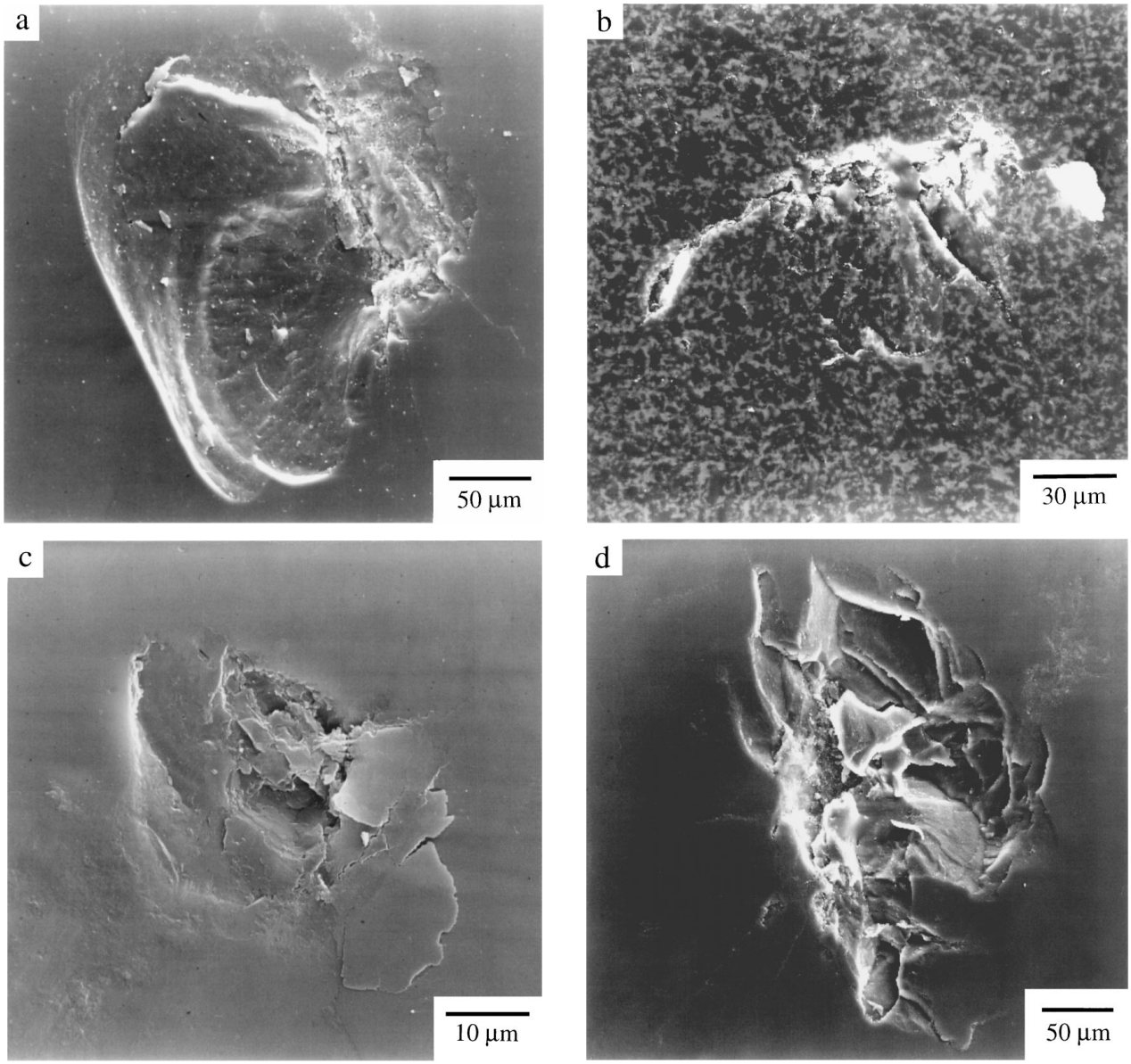

Figure 4 Single impact damage produced from impacts by 600 μm silicon carbide at 93 m/s: (a) BC10B, (b) BCSiSiC, (c) BC60B and (d) MBC60B. Note the difference in magnification between the micrographs.

small addition of boron is facilitates material transport and thereby reduces the porosity.

To introduce boron may also be a strategy to reduce the content of free graphite in the microstructure. Carbon and boron recombine during sintering to produce boron carbide. In addition, the free carbon may be reduced by the carbon enrichment of the boron carbide phase. However, initially the boron carbide is at the carbon rich limit and therefore no carbon enrichment of the boron carbide phase is possible. During sintering extensive diffusion of boron and carbon within the material takes place. It has been shown that the boron supply to the carbide phase is higher than the carbon supply to the boron phase [24] and therefore an excessive addition of boron will be necessary to eliminate a lowresidual content of carbon. This demonstrates the relatively high levels of retained graphite in the mould injected MBC60B specimen, in which the binder contributes to the higher content of free graphite. The decreasing grain size with increasing boron addition up to 20 wt.% is presumably due to the increased propensity of grain nucleation as free carbon and boron recombine to form boron carbide.

A very low fraction of porosity was obtained in the materials produced from powder containing 60 wt.% B. The unit cell increases with the boron content (Table III), which is in agreement with observations of Bouchart and Thevenot in [5]. Therefore, boron enrichment of the boron carbide causes an extensive swelling within the material that also increases the driving force of the sintering process. This contributes to the reduction of the closed porosity, leading to an almost pore free material. The increased densification is, unfortunately also associated with a partially substantial grain growth, se Table I.

An additive that promotes liquid phase sintering may lead to the elimination of porosity. The liquid phase aid the sintering through two mechanisms: (i) it promotes densification by activated sliding and (ii) by a solution-reprecitation mechanism which enhance diffusion by transport of the sintering material as a solute in the liquid phase. Silicon has a good chemical affinity in the

B-C system with the formation of stable phases such as silicides and silicon carbides. According to earlier reports [25] liquid silicon forms a low wetting angle of 20° on boron carbide. This was accompanied by a reaction between the liquid silicon and the boron carbide leading to the formation of β-SiC in the contact zone; the crystals grow by recrystallization trough the liquid phase. It has also been reported [26] that silicon can be introduced and exchanged for boron and carbon atoms in the row of interstitial atoms, with a maximum solubility limit of 2%. However, as the composition of the used boron carbide powder is at its carbon solubility limit, $B_{4.0}C$, no exchange or dissolution of boron from the row of interstitial atoms is possible. Therefore, only an extensive carbon diffusion can takes place within the material during the sintering. Thus, the reaction with pure silicon produces only silicon carbide for moderate amounts of Si.

4.2. Particle erosion

The primary erosion mechanism of all the materials appears to be removal of material by lateral cracks that intersect the surface. A secondary substantial mechanism of material removal is due to the removal of whole grains as a result of intergranular cracks originating from weak spots at the surface, such as weak grain boundaries, pores or graphite inclusions. Intergranular cracks may also be initiated at the lateral cracks, which forms due to the elastic-plastic zone beneath the impinging particles. In addition there are internal stresses in the grain boundaries due to lattice mismatch, and phase transformations due to the boron enrichment.

Adding silicon and/or silicon carbide to boron carbide appears to be a strategy for improved erosion resistance. The erosion rates of the BCSi and BCSiSiC were less than half of that for the pure BC specimen. This is probably due to a combination of strengthening of grain boundaries as a consequence of improved sintering and the very low porosity. In addition, the transformation of Si and C into SiC reduced the quantity of graphite in the grain boundaries. Presence of SiC at grain boundaries makes these regions less prone to brittle cracking. This may be a consequence of the excellent chemical affinity between the SiC phase and the boron carbide, which results in a strong bond by surface chemical reaction, as outlined in [25, 26]. In addition, the silicon carbide phase may reduce the impact damage by transferring the energy from external impacts to surrounding material and by partial consumption of the impact energy.

It is an interesting observation that additions up to 20 wt.% B had no obvious effect on the wear resistance, although the closed porosity was decreased significantly in comparison to that of BC, see Table I. Superior resistance followed by the very low porosity and absence of graphite inclusions in BC60B to erosion. The deteriorating effects of graphite inclusions can be illustrated by comparing the wear resistance and the single impacts of the BC60B (Fig. 4c) specimen to that of the mould injected MBC60B specimen with some residual graphite (Fig. 4d). Observations of the single impacts on the latter material showed that approximately 20% of the lateral fractures were considerably larger. These impact sites were probably a result of individual strikes on or near graphite inclusions. An added factor could be the strain accommodation provided by the boron enrichment.

Smearing of SiC onto the eroded surfaces was observed. This may have contributed to a more plastic appearance of some surfaces, such as in Fig. 3c. SEM micrographs of the single impacts show no evidence of plastic deformation, but instead supports that particle fragmentation occurs since it was observed that some of the erodent adhered to the impact site, see Fig. 4c.

The results of the hardness and fracture toughness testing appear to produce conflicting results to the erosive wear tests. In the microstructure study it is demonstrated that defects such as pores, graphite inclusions and weak grain boundaries may act as stress concentrators where cracks can initiate. This will especially be evident during continuous striking as a result of fatigue. However, in fracture toughness tests where a crack propagates rapidly from the corners of a Vickers impression the defects in the sample surface has much less influence on the K_c value. In this test, graphite inclusions and grain boundaries may instead arrest cracks [27].

The importance of the relative hardness between the erodent and the target has been frequently discussed in the literature [28, 29]. Boron carbide is considerably harder than silicon carbide. The SEM examination of the single impact sites indicates that particle crushing occurred since some of the crushed erodent adhered to the impact site. With softer erodents it would have been reasonable to expect a less brittle mechanism of material removal. However, the micrographs of the impact damages present no evidence of such a change of material removal. Similar observations have been made by a number of investigators [29–31]. Scattergood and coworkers [29] concluded that the mechanism is the same, but more damage accumulation for softer erodents are necessary to build up the required stresses to produce lateral cracks. Therefore, the greatly improved erosion resistance of the CIP produced boron carbide containing 60 wt.% boron is probably due to the absence of weak fracture initiating spots in the surface such as weak grain boundaries, pores and graphite inclusions.

5. Conclusions

– The addition of large amounts of boron improves the erosion resistance of boron carbide. It is suggested that this is a result of the elimination of porosity and graphite inclusions.

– The erosive wear resistance is also substantially improved by introducing silicon carbide as a grain boundary phase.

– Boron enrichment of the boron carbide causes enlargement of its unit cell, which facilitates the densification.

– Removal of graphite in the grain boundaries with large additions of boron leads to grain growth.

Acknowledgements

The Swedish Research Council for Engineering Sciences (TFR) and AC Cerama AB are acknowledged for their financial support and for providing the samples, respectively.

References

1. G. DE WITH, *J. Less Common Met.* **95** (1983) 133.
2. F. THEVENOT, *J. Euro. Ceram. Soc.* **6** (1990) 205.
3. A. G. EVANS, M. E. GULDEN and M. ROSENVLATT, *Proc. R. Soc. Lond.* **A361** (1978) 343.
4. A. W. RUFF and S. M. WIEDERHOLM, "Treatise on Materials Science and Technology," Vol. 16 (Academic Press, New York, 1979) p. 69.
5. M. BOUCHACOURT and F. THEVENOT, *J. Less Common Met.* **82** (1981) 227.
6. E. AMBERGER, M. DRUMINSKY and K. PLOOG, *ibid.* **23** (1971) 43.
7. L. B. EKBOM, B. LARS and C. O. AMUNDIN, *Science of Ceramics* **11** (1981) 237.
8. K. PLOOG, *J. Less Common Met.* **35** (1974) 115.
9. K. A. SCHWETZ and G. W. GRELLNER, *ibid.* **82** (1981) 37.
10. C. GRESKOVICH and L. H. ROSOLOWSKI, *J. Am. Ceram. Soc.* **59** (1976) 336.
11. S. L. DOLE and S. PROCHAZKA, *Ceram. Eng. Sci. Proc.* **6** (1985) 1151.
12. S. L. DOLE, S. P. PROCHAZKA and R. H. DOREMUS, *J. Am. Ceram. Soc.* **72** (1989) 958.
13. T. LARKER, *Mater. Sci. Eng.* **71** (1985) 329.
14. ASTM Designation: E562-83, "Standard Practises for Determining the Volume Fraction by Sytematic Manual Point Count".
15. J. C. WURST and J. A. NELSON, *J. Am. Ceram. Soc.-Discussion and Notes* **55** (1972) 109.
16. S. SÖDERBERG, S. HOGMARK, U. ENGMAN and H. SWAHN, *Trib. Int.* **16** (1981) 333.
17. C. B. PONTON and R. D. RAWLINGS, *Mater. Sci. Technol.* **5** (1989) 865.
18. *Idem., ibid.* **5** (1989) 961.
19. F. THÉVENOT, *J. Nuclear Mater.* **152** (1988) 154.
20. H. SUZUKI *et al.*, *Yogyo-Kyokai* **87** (1979) 430.
21. F. THEVENOT and M. BOUGOIN, in AIP Conference Proceeding, Abuquerque, June 1986, edited by D. Emin (American Institute Physics, New York) p. 51.
22. B. L. GRABCHUK and P. S. KISLEY, *Poroshkovaya-Metallurgya* **15** (1976) 18.
23. *Idem.*, (Translation) *ibid.* **165** (1976) 18.
24. M. BOUCHACOURT, C. BRODHAG and F. THEVENOT, *Science of Ceramics* **11** (1981) 231.
25. A. D. PANASYUK, V. D. ORESHKIN and V. R. MASLENNIKOVA, *Poroshkovaya Metallurgiya* **199** (1979) 79.
26. L. B. EKBOM, *Science of Ceramics* **9** (1977) 183.
27. J. W. HUTCHINSON, *Acta Metall.* **23** (1987) 1605.
28. P. H. SHIPWAY and I. M. HUTCHINGS, *Wear* **149** (1991) 85.
29. J. L. ROUTBORT and R. O. SCATTERGOOD, *Key Eng. Mater.* **71** (1992) 23.
30. L. MURUGESH, S. SRINIVASAN and R. O. SCATTERGOOD, *J. Mater. Eng.* **13** (1991) 55.
31. E. NESS and R. ZIBBELL, *Wear* **196** (1996) 120.

Received 15 November
and accepted 14 December 1999